

FeCl₃ doped polyvinylidene fluoride

Part II *Pauli susceptibility and microwave response*

A. TAWANSI, H. I. ABDEL-KADER, W. BALACHANDRAN*, E. M. ABDEL-RAZEK
Physics Department, Faculty of Science, Mansoura University, Mansoura, 35516, Egypt
 *Department of Electronic and Electrical Engineering, University of Surrey, Guilford, Surrey,
 GU2 5XH, UK

Magnetic susceptibility measurements of FeCl₃ doped polyvinylidene fluoride (PVDF) films over the dopant mass fraction range $0 \leq W \leq 0.45$ (wt %) and the temperature, T , range 85–300 K are presented. Undoped PVDF exhibited temperature independent Pauli paramagnetic (TIPP) susceptibility at $150 \leq T \leq 300$ K, which was followed by an antiferromagnetic Neel peak at $T_N = 120$ K. In the case of doped PVDF, TIPP susceptibility was followed by a Curie–Wiss temperature dependence with a positive paramagnetic Curie point, indicating ferromagnetic interaction at lower temperatures. The onset of TIPP was attributed to one-dimensional magnetic interaction of itinerant states close to the Fermi surface. It is implied that the $[\text{C}_2\text{H}_2\text{F}_2(\text{FeCl}_4)_y(\text{FeCl}_2)_z\text{Cl}_z]_x$ complex was formed by doping. A chlorination model was proposed to calculate the stoichiometric coefficients y and z , using magnetic susceptibility data. The microwave response of the doped PVDF has been examined. It is found that changing the doping level results in composites of different reflection coefficient phase and power reflection factors.

1. Introduction

It has been reported that [1] doped organic polymers display phenomena which are in some ways similar to conventional semiconductors, and which were therefore described theoretically in early works as usual doped inorganic semiconductors with rigid band models. However, these polymers possess highly anisotropic interaction, which can lead to collective instabilities typical of quasi-one-dimensional materials, such as Peierls–Frölich modes. Furthermore, because these polymers are organic compounds, it can be anticipated that electronic excitations or charge transfer processes will markedly affect the atomic geometry; just as in typical organic molecules, important effects due to electron–phonon coupling are, therefore, expected. From Hartree–Fock self-consistent field calculations on trans-polyacetylene (TPA), poly-paraphenylene and polypyrrole, Brédas *et al.* [1] demonstrated that charge transfer induces dramatic geometric modifications on the polymeric chain. These modifications in turn lead to the appearance of electronic states in the gap, that are predicted to play major roles in the conductivity mechanism and in the magnetic properties of polymers. It is found that the geometry of each defect strongly depends on its charge state, and that lattice relaxation around the defect is spatially less extended than the polarization cloud (spin density wave or charge density wave) that the defect induces.

In a previous work [2] infrared (i.r.) and optical transmittance spectra, differential thermal analysis

(DTA) and d.c. electrical resistivity of FeCl₃ doped polyvinylidene fluoride (PVDF) films, over the doping mass fraction range $0 \leq w \leq 0.4$ has been studied. The i.r. spectra provided evidence of the presence of: (a) both α and γ crystalline phases for the undoped PVDF, and a γ phase for the doped films; (b) a head-to-head (h-to-h) or tail-to-tail (t-to-t) content of 20%; and (c) a different doping mode beyond the 0.25 doping level. Optical spectra suggested two induced energy bands, in the energy gap of the studied composite, and a probable interband electronic transition. A (doping) dipole relaxation and a premelting point were identified by two endothermic DTA peaks (typically at 320 and 443 K, respectively) for the 0.35 wt % FeCl₃ doping level. Temperature dependence of the d.c. resistivity of the doped PVDF was attributed to inter-polaron hopping among the polaron and bipolaron states, induced by doping. The calculated hopping distances (≤ 0.13 nm) were too small to be along the CC sites. Thus, conduction is of interchain type, through the dopant sites. On the other hand, Das-Gupta *et al.* [3] found that, for the undoped PVDF, the obtained jump distance of the charge carrier (~ 0.25 nm) equals the separation of two successive h-to-h (or t-to-t) defects. These defects, accordingly, were considered to be jumping sites for charge carriers, and conduction was therefore of intrachain type.

As far as is known, the magnetic properties of PVDF have not yet been studied. Thus, the present work is devoted to an investigation of the effect of

FeCl₃ doping on the magnetic properties and microwave response of PVDF. This is done for the sake of finding probable magnetic and microwave applications of doped PVDF films.

2. Experimental procedure

Samples were made from α -PVDF resin provided by Solvay (Belgium) and referenced as: SOLEF 1008. Dimethylformamide was used as a solvent for the resin, and FeCl₃ as the dopant. Films were prepared by casting the desired solution onto glass, such that the films were approximately 0.2–0.5 mm thick after the solvent was removed at 343 K. Magnetic susceptibility was measured using the Faraday pendulum balance technique, with accuracy better than $\pm 3\%$. Diamagnetic corrections were done. To investigate the microwave response of the prepared films, a standing wave experiment was used. The apparatus was of type KDR-10SA crystal mount (ANDO Electrical Co., Japan). Experiments were made in the 10 GHz band, with WRJ-10 wave guides and BRJ flanges (both according to JIS standards). The sample was connected, as a load, to the receiving end of the microwave line. Let the detected maximum and minimum values of the d.c. current by I_1 and I_2 ; then, the standing wave S ratio is

$$S = (I_1/I_2)^{1/2} \quad (1)$$

3. Results and discussion

3.1. Undoped PVDF

Fig. 1 shows the temperature dependence of magnetic susceptibility, χ , of the undoped PVDF in the temperature range 85–300 K. A temperature independent Pauli paramagnetic susceptibility, χ_p , is observed in the range 150–300 K, with a slight step transition at 253 K. This step transition is close to the previously observed thermally stimulated discharging current peak at $T_\alpha = 253$ K [4, 5], which was attributed to α_c relaxation of dipoles in the PVDF crystalline phase [6, 7]; the dipoles are situated at the folds of the molecular chains [8]. Moreover, in Fig. 1, a clear Neel antiferromagnetic peak is observed at $T_N = 123$ K, which is followed by an increasing susceptibility value for a further decrease in T .

The observed results suggest a linear chain (one-dimensional) character in the Pauli paramagnetic region due to itinerant states, forming an energy band in the vicinity of the Fermi level, E_F [9–11]. The peak at T_N may have arisen from two-dimensional antiferromagnetic interaction [12], which is followed by another three-dimensional antiferromagnetic interaction for a further decrease in T [13]. These antiferromagnetic interactions may be taken as evidence for the coexistence of some localized energy states, together with the previously mentioned itinerant ones [14]. The one-, two-, three-dimensional sequence of magnetic interactions, due to cooling, implies anisotropic distribution (AD) of the magnetic sites in PVDF. This AD may be due to: (a) lattice anisotropy of the α and γ phases, where the lattice constants are such that $b > c > a$, and c is parallel to the chain axis [15–17]; and (b) the presence of 20% h-to-h (or t-to-t) defects, i.e. this defect is repeated at each five carbon atoms along the chain [2, 18].

The magnetic sites in PVDF are thought to be of a spin polaron type. This may be explained as follows. Das-Gupta *et al.* [19] showed that, for PVDF, the charge lying on the crystal surface (of average linear dimension = 20 nm) is $\sim 10^{-19}$ C, i.e. an electronic charge. Using this result and assuming the separation between two successive h-to-h (or t-to-t) defects to be ~ 1.25 nm, the average charge transfer per h-to-h defect was found to be $\sim 2.44 \times 10^{-4}$ e. The presence of a charge transfer at the h-to-h and t-to-t defects is supported by peaks in potential energy distribution along the chain, obtained at h-to-h and t-to-t defects by Kobayashi *et al.* [18]. This allows for the formation of polarons at the h-to-h and t-to-t defects. Polarons can also arise from [20] the bonding interaction conjugation sequence of pi molecular orbitals (MOs). Moreover, interchain interaction between the delocalized (positive or negative) polaron, involving pi MOs (of appropriate symmetry) and the alternant non-classical polymeric fragments [21], may result in a macroscopic magnetic property throughout a piece of polymer. The partly populated MOs formed, will develop into a band by further interaction with polarons on adjacent chains. Hence, the Pauli magnetic susceptibility will increase as the polaron concentration increases. Thus, it is believed that the one-dimen-

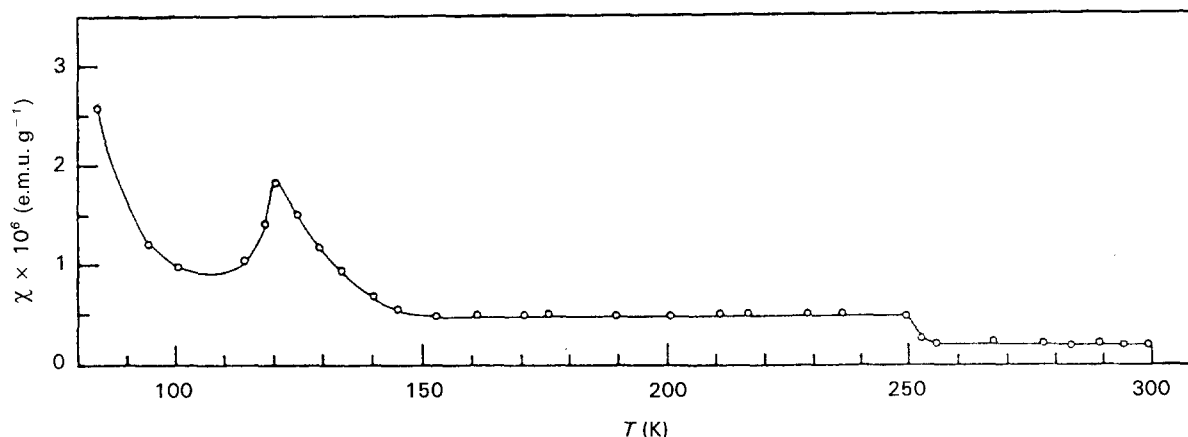


Figure 1 Temperature dependence of magnetic susceptibility for undoped PVDF films.

sional magnetic interaction spin polaron lies along the (shortest) lattice constant a , and two-dimensional interaction is through the a - c plane.

3.2. FeCl₃ doped PVDF

Fig. 2a, b depicts the temperature dependence of the susceptibility reciprocal of PVDF doped with various mass fractions, w , of FeCl₃, where $0.05 \leq w \leq 0.45$. The obtained plots are characterized by a TIPP susceptibility down to a critical temperature, T_c , below which χ exhibits Curie-Weiss behaviour with a positive paramagnetic Curie point, θ_p , indicating ferromagnetic interaction in the low temperature region. Thus, as the temperature decreases, one-dimensional (itinerant state) magnetic interaction is transformed directly, at $T < T_c$, to a three-dimensional (localized state) interaction.

Fig. 3 shows the effect of the dopant mass fraction on T_c , θ_p and χ_{120} (measured at 120 K). It is clear that increasing w up to 0.25 does not influence the T_c value. On the other hand, T_c decreases linearly as w increases beyond 0.30. A broad maximum is observed for each θ_p and χ_{120} value around the critical dopant level, $w_c (= 0.30)$. Since all the doping levels for the present material are in the paramagnetic state, the decrease in

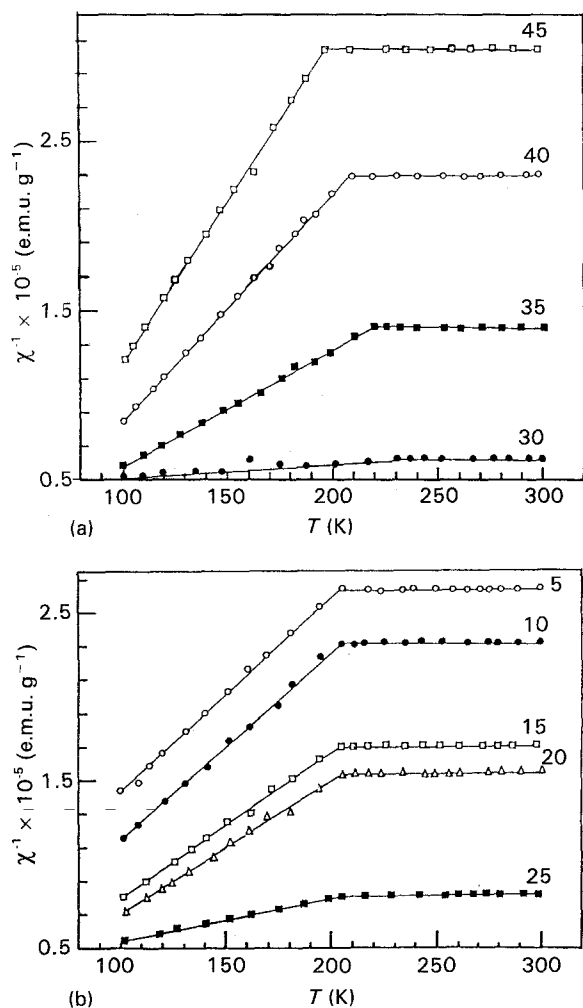


Figure 2 χ^{-1} versus T for PVDF doped with (a): (○) 5, (●) 10, (□) 15, (Δ) 20 and (■) 25 wt % FeCl₃; (b): (●) 30, (■) 35, (○) 40 and (□) 45 wt % FeCl₃.

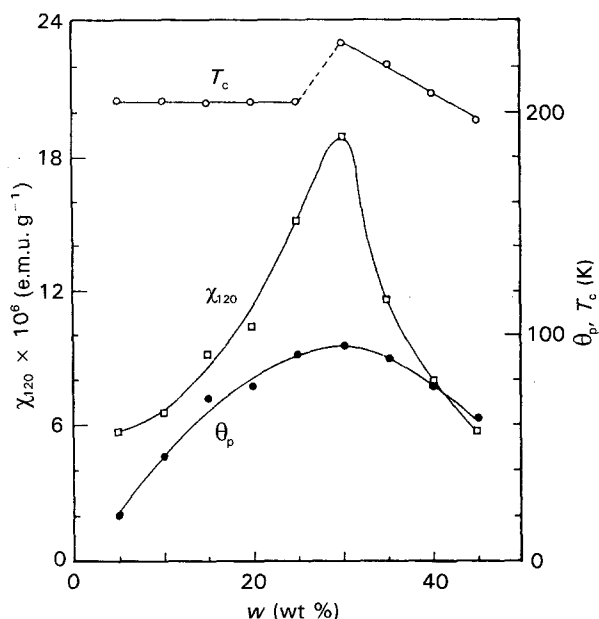


Figure 3 Dependence of χ_{120} , θ_p and T_c on dopant fraction.

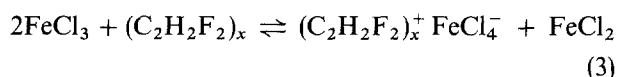
χ_{120} and θ_p for $w > w_c$ indicates a limiting dopant state and the onset of a new-impeding mechanism. Attempting to understand the doping mechanisms for each stage, one may proceed as follows.

The Pauli paramagnetic susceptibility can be represented as

$$\chi_p = \mu_B^2 N(E_F) \quad (2)$$

where μ_B is the Bohr magneton and $N(E_F)$ is the density of states at the Fermi surface for both spins (in units of states per unit energy per carbon atom). The density of states for the undoped and doped PVDF samples are calculated, using Equation 2 and the experimental values of χ_p . The obtained results are normalized to the undoped values $N_o(E_F)$ and the values of $\log[N(E_F)/N_o(E_F)]$ are plotted versus w in Fig. 4. A linear increase is noticed for $\log[N(E_F)/N_o(E_F)]$ as a function of w up to a maximum value at w_c , above which the same function decreased linearly.

Motivated by the analogy of dopants of polyacetylene with various transition metal halides [22] and by the results of Pron *et al.* [23], that the efficient electron acceptor FeCl₃ takes two electrons from polyacetylene forming a bivalent high spin anion FeCl₄⁻, for doping PVDF the following dismutation reaction [24] is assumed.



According to Equation 3 magnetic susceptibility of PVDF doped with w (wt %) FeCl₃ can be expressed as

$$\chi_{il} = \frac{1}{M_p(1+w)} \left[\chi_p + \frac{w}{2} M_p \left(\frac{\chi_1}{M_1} + \frac{\chi_2}{M_2} \right) \right] \quad (4)$$

where M_p and χ_p , M_1 and χ_1 , and M_2 and χ_2 are the molar mass and (magnetic susceptibility) of undoped PVDF, FeCl₄ and FeCl₂, respectively; and $\chi_1 = 13430.243 \times 10^{-6}$ e.m.u. mol⁻¹ and $\chi_2 = 12828 \times 10^{-6}$ e.m.u. mol⁻¹ [25].

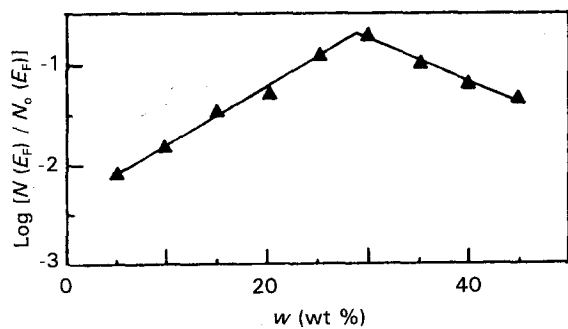


Figure 4 The effect of w on the logarithm of the normalized density of states at the Fermi surface.

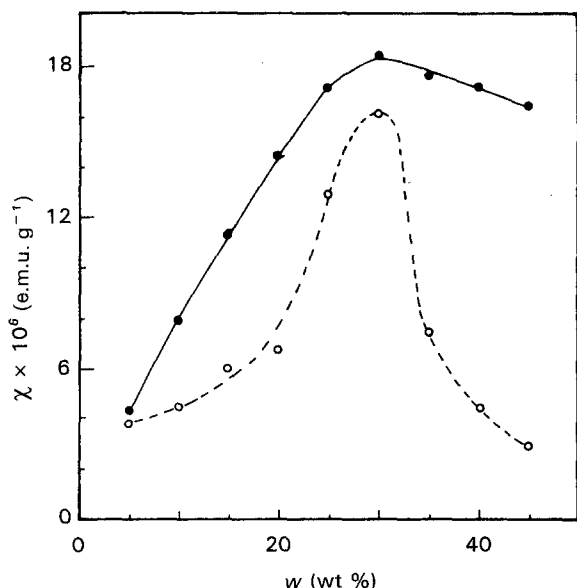


Figure 5 The effect of dopant fraction on χ : (○) obtained experimentally, and (●) calculated using Equations 4 and 5.

However, Fig. 5 shows that the experimental values of room temperature susceptibility exhibits a peak at $w_c = 0.30$ FeCl₃. This behaviour may be explained if one assumes a maximum FeCl₃ insertion level and continuous chlorination, which follows this limiting intercalation level. Hence, the observed decay of χ arose from insertion of diamagnetic chlorine instead of paramagnetic FeCl₄⁻, assuming that chlorine forms a covalent bond with the polymer chain and no more FeCl₄⁻ is inserted above w_c ($= 0.30$ corresponding to 0.059 FeCl₄⁻ per C₂H₂F₂ unit). Thus, the following formula can be used for susceptibility at high dopant levels ($w > 0.30$), [26]

$$\chi_{ih} = \frac{1}{M_P(1+w)} \left\{ \chi_P + M_P \left[0.15 \left(\frac{\chi_1}{M_1} + \frac{\chi_2}{M_2} \right) + (w - 0.3) \frac{\chi_3}{M_3} \right] \right\} \quad (5)$$

where χ_3 and M_3 are the susceptibility and molar mass of chlorine, and $\chi_3 = -20.1 \times 10^{-6}$ e.m.u. mol⁻¹ [25]. In Fig. 5 the continuous and dashed curves represent susceptibility calculated according to Equations 4 and 5, respectively. It is remarkable that the experimental data are of lower values than the calculated ones for all doping levels. This observation may be attributed

to one (or both) of the following reasons: (a) there is magnetic interaction between the dopant sites and neighbouring spin polarons, formulated previously by Hudak [27] and Tawansi *et al.* [28]; (b) further chlorination may take place even at the lowest FeCl₄⁻ insertion level. Therefore, modifying Equations 4 and 5, to include correction factors for assumed further chlorination, Equations 6 and 7 are derived as follows

$$\chi_{ext} = \frac{1}{M(1+w)} \left\{ \chi_P + M_P \left[\left(\frac{w - w_3}{2} \right) \times \left(\frac{\chi_1}{M_1} + \frac{\chi_2}{M_2} \right) + w_3 \frac{\chi_3}{M_3} \right] \right\} \quad (6)$$

$$\chi_{exh} = \frac{1}{M(1+w)} \left\{ \chi_P + M_P \left[\left(\frac{w - w_3}{2} \right) \times \left(\frac{\chi_1}{M_1} + \frac{\chi_2}{M_2} \right) + (w - w_3 - 0.30) \frac{\chi_3}{M_3} \right] \right\} \quad (7)$$

where w_3 is the mass fraction of chlorine due to assumed further chlorination.

The above discussion implies that FeCl₄ doping of PVDF leads to the formation of a complex with the following form [C₂H₂F₂(FeCl₄)_y(FeCl₂)_zCl_x]. The stoichiometric coefficients y and z are calculated for our samples using the magnetic data and Equations 4–7; the results are shown in Fig. 6. It is noticed that the maximum content of FeCl₄⁻ corresponds to the composition [C₂H₂F₂(FeCl₄⁻)_{0.059}(FeCl₂)_{0.059}Cl_{0.15}]. Further chlorination would then involve the elimination of FeCl₄⁻. This assumption agrees with the observed slight decay of the y coefficient for $w > 0.30$, while the z value increases monotonically.

The magnetic moments, μ_1 and μ_2 per FeCl₄ and FeCl₂ molecules, respectively, are calculated according to the formula

$$\mu = 2.839(\chi_m T)^{1/2} \quad (8)$$

where χ_m is the corresponding molar susceptibility, with a molar fraction y , at 120 K. The values of μ_1 , μ_2 and of the total magnetic moment, $\mu_T = \mu_1 + \mu_2$ are plotted as functions of the dopant mass fractions, in Fig. 7. It is remarkable that the maximum values of μ_1 and μ_2 (2.41 μ_B and 3.01 μ_B , respectively) are smaller than the theoretical (4.9 μ_B) and experimental (5.1–5.5 μ_B) values found in the literature for Fe²⁺ ions [25].

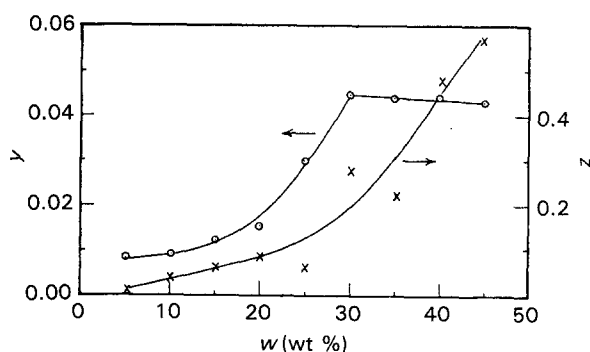


Figure 6 Calculated stoichiometric parameters y and z at various doping fractions.

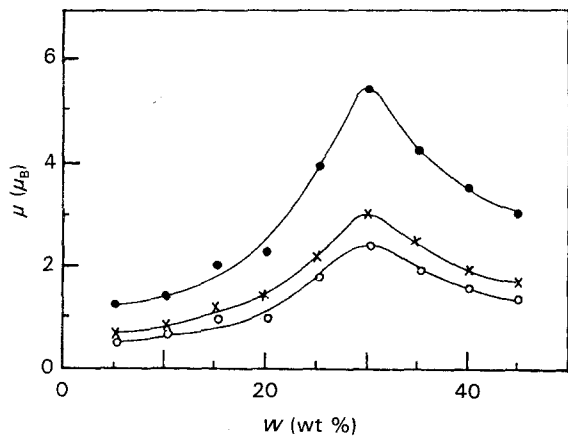


Figure 7 The effect of doping fraction on: (o) the magnetic moment (μ_1) per FeCl_4 , and (x) μ_2 per FeCl_2 molecule, and (●) total magnetic moment, μ_T .

This discrepancy may be attributed to the influence of the chlorine bridge on the Fe^{2+} states in FeCl_4^- and FeCl_2 cases. Moreover, if the differences between the theoretical and present experimental values of μ_1 and μ_2 are denoted by $\Delta\mu_1$ and $\Delta\mu_2$, respectively, then $\Delta\mu_1/4$ and $\Delta\mu_2/2$ represent the decrease in the magnetic moment per chlorine ion in each case. Typical values of $\Delta\mu_1/4$ and $\Delta\mu_2/2$, at the critical dopant fraction, are 0.62 and 0.94 μ_B , respectively. These results suggest different modes of chlorine bridges for FeCl_4^- and FeCl_2 in the present composites [29].

3.3. Microwave response

To investigate the effect of doping level on microwave response, a standing wave experiment was used. In this experiment, the value of the reflection coefficient is defined as

$$R = \frac{\text{reflected wave voltage}}{\text{incident wave voltage}} = \frac{S - 1}{S + 1} \quad (9)$$

and the phase is

$$\phi = (4\pi d/\lambda) - \pi \quad (10)$$

where S is the standing wave ratio defined in Equation 1, λ is the wavelength and d is the location of the first minimum of the standing wave apart from the load terminal side of the wave guide. The power reflection, Pr , factor is given by

$$Pr = \left(\frac{S - 1}{S + 1} \right)^2 = R^2 \quad (11)$$

The obtained values of ϕ and Pr are plotted versus the dopant mass fraction in Fig. 8. It is found that the doping level affects ϕ in a similar manner to that of the hopping distance, R_0 , in electrical conduction reported in Reference [2]. This result indicates that the obtained microwave phase is affected mainly by the concentration of impurity states in the studied films. On the other hand, the observed peak of $\log Pr$ as a function of dopant content is nearly similar to the susceptibility behaviour. Hence, it is implied that the major influence on the power reflection factor is

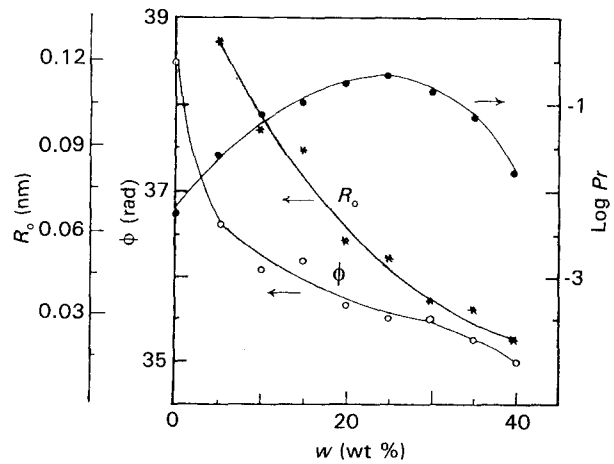


Figure 8 Dopant fraction dependence of (o) the phase of the microwave reflection coefficient ϕ , (●) the logarithm of its power reflection factor, Pr , (*) the inter-polaron hopping distance R_0 [2].

the magnetic state of the film. Moreover, Fig. 8 shows that by changing the doping level of PVDF, one may find two composite films of different ϕ values, but having the same Pr value. This suggests an important application of the present samples in microwave cavities and antennae.

4. Conclusions

Magnetic measurements gave evidence for the coexistence of localized and itinerant magnetic energy states in the undoped PVDF due to spin polarons. Both types of energy states are influenced by the FeCl_3 doping level. It is implied that the impurity states of electric activity, induced by doping, are different from the magnetic ones.

The suggested chlorination model allowed interpretation of the dependence of κ on w , and calculation of the stoichiometric coefficients y and z of the proposed complex $[\text{C}_2\text{H}_2\text{F}_2(\text{FeCl}_4)_y(\text{FeCl}_2)_z\text{Cl}_z]_x$ at various doping levels.

The present composites can be used in microwave technology.

References

1. J. L. BRÉDAS, B. THÉMANS, J. M. ANDRÉ, R. R. CHANCE, D. S. BOUDREAUX and R. SILBEY, *J. De Physique* **44** (1983) 373.
2. A. TAWANSI, H. I. ABDEL-KADER, M. EL-ZALABANY and E. M. ABDEL-RAZEK, *J. Mater. Sci.* (1993) Part I of this paper, in press.
3. D. K. DAS-GUPTA, K. DOUGHTY and R. S. BROEKLEY, *J. Phys. D: Appl. Phys.* **13** (1980) 2101.
4. P. HEDVIG, "Dielectric Spectroscopy of Polymers" (Adam Hilger, Bristol, 1977) p. 76.
5. S. ELIASSON, *J. Phys. D: Appl. Phys.* **18** (1985) 275.
6. T. MIZUTANI, T. YAMADA and M. IEDA, *ibid.* **14** (1981) 1139.
7. Y. OKA and N. KOIZUMI, *Polym. J.* **14** (1982) 869.
8. D. K. DAS-GUPTA and K. DOUGHTY, in Proceedings of the International Conference on Dielectric Materials (Institute of Electrical Engineers, Conference Publication No. 177, 1979) p. 242.
9. B. R. WEINBERGER, J. KAUFER, A. J. HEEGER, A. PRON and A. G. MacDIARMID, *Phys. Riv. B.* **20** (1979) 1.
10. A. TAWANSI and H. M. ZIDAN, *J. Phys. D: Appl. Phys.* **23** (1990) 1320.

11. *Idem.*, *Int. J. Polym. Materials* **15** (1991) 77.
12. L. O. SNIVELY, P. I. SERIFERT, K. EMERSON and J. E. DRUMHELLER, *Phys. Riv. B* **20** (1979) 2101.
13. H. KOBAYASHI, T. HASEDA, E. KANDA and S. KANDA, *J. Phys. Soc. Japan* **18** (1963) 349.
14. S. ROTH, K. EHINGER, K. MENKE, M. PEO and R. J. SCHWEIZER, *J. De Physique* **44** (1983) C 3-69.
15. R. HASEGAWA, M. KOBAYASHI and H. TADOKORO, *Polym. J.* **3** (1972) 591, 600.
16. A. J. LOVINGER, in "Developments in Crystalline Polymers", Vol. 1, edited by D. C. Bassett (Applied Science, London, 1982) Chapter 5.
17. R. ZHANG and P. L. TAYLOR, *J. Chem. Phys.* **94** (1991) 3207.
18. M. KOBAYASHI, K. TASHIRO and H. TADOKORO, *Macromol.* **8** (1975) 158.
19. D. K. DAS-GUPTA and K. DOUGHTY, *Appl. Phys. Lett.* **31** (1977) 585.
20. A. G. MacDIARMID and T. C. CHUNG, *J. De Physique* **44** (1983) 513.
21. N. N. TYUTYULKOV, O. E. POLANSKY, P. SCHUSTER, S. H. KARABUNARLIV and C. I. IVANOV, *Theoret. Chem. Acta* **67** (1985) 211.
22. H. SHIRAKAWA and T. KOBAYASHI, *J. De Physique* **44** (1983) C 3-3.
23. A. PRON, D. BILLAUD, I. KULSZEWICZ, C. BUDROWSKI, J. PRZYLUKSI and J. SUQALSKI, *Mater. Res. Bull.* **16** (1981) 1229.
24. F. BENIERE and S. PEKKER, *Solid State Commun.* **57** (1986) 835.
25. G. FOEX, "Constanes Selectionees de Dia et Paramahnetisme" (Masson, Paris, 1957) p. 103.
26. S. FLANDROIS, A. BOUKHARI, A. PRON and M. ZAGORSKA, *Solid State Commun.* **67** (1988) 471.
27. O. HUDAK, *Czech. J. Phys. B* **35** (1985) 1303.
28. A. TAWANSI, N. KINAWY and M. EL-MITWALLY, *J. Mater. Sci.* **24** (1989) 2497.
29. N. T. ABDEL-GHANI, A. TAWANSI and S. A. ABDEL-LATIF, *Bull. Soc. Chem. Fr.* **127** (1990) 188.

*Received 11 May
and accepted 10 December 1993*